Agricultural Water Management 221 (2019) 13–24

Contents lists available at ScienceDirect

Agricultural Water Management

journal homepage: www.elsevier.com/locate/agwat

Simulating the impacts of climate change on hydrology and crop production in the Northern High Plains of Texas using an improved SWAT model

Yong Chen[a,*], Gary W. Marek[b], Thomas H. Marek[c], Jerry E. Moorhead[b], Kevin R. Heflin[c], David K. Brauer[b], Prasanna H. Gowda[d], Raghavan Srinivasan[a]

[a] Department of Ecosystem Science and Management, Texas A&M University, 2138 TAMU, College Station, TX 77843, USA
[b] USDA-ARS Conservation and Production Research Laboratory, 300 Simmons Rd., Unit 10, Bushland, TX 79012, USA
[c] Texas A&M AgriLife Research, Texas A&M AgriLife Research and Extension Center, 6500 Amarillo Blvd W, Amarillo, TX 79106, USA
[d] USDA-ARS Grazinglands Research Laboratory, 7207 West Cheyenne Street, El Reno, OK 73036, USA

ARTICLE INFO

Keywords:
Dryland
Fallow
General circulation model (GCM)
Irrigation
Evapotranspiration
Yield

ABSTRACT

Modeling the effects of climate change on hydrology and crop yield provides opportunities for choosing appropriate crops for adapting to climate change. In this study, climate change impacts on irrigated corn and sorghum, dryland (rainfed) sorghum, and continuous fallow in the Northern High Plains of Texas were evaluated using an improved Soil and Water Assessment Tool (SWAT) model equipped with management allowed depletion (MAD) irrigation scheduling. Projected climate data (2020–2099) from the Coupled Model Intercomparison Project Phase 5 (CMIP 5) of 19 General Circulation Models (GCMs) were used. Climate data were divided into four 20-year periods of near future (2020–2039), middle (2040–2059), late (2060–2079), and end (2080–2099) of the 21st century under two Representative Concentration Pathway (RCP) emission scenarios (RCP 4.5 and RCP 8.5). For irrigated corn, median annual crop evapotranspiration (ET) and irrigation decreased by 8%–25% and 15%–42%, respectively, under the climate change scenarios compared to the historical period (2001–2010). The median yield was reduced by 3%–22% with exponentially decreases in the latter half of the 21st century. For sorghum, the reduction of median annual crop ET ranged from 6%–27%. However, the decline in the median annual irrigation was within 15%, except for the 2060–2079 and 2080–2099 periods under RCP 8.5 scenarios with 30% and 49% reductions in median annual irrigation. The median irrigated sorghum yield declined by 6%–42%. The median annual crop ET of dryland sorghum decreased by 10%–16%. The reduction in median yield was within 10% of the historical dryland sorghum yield. The decrease in median annual evaporation varied from 15%–23% under future continuous fallow conditions. The elevated CO_2 level of future climate scenarios was the primary factor for the decrease in the ET and irrigation. The reduction in future crop yield was mainly attributed to the shortening of the maturity period caused by increased future temperature.

1. Introduction

Increasing combustion of fossil fuels leads to the rise of atmospheric CO_2 concentration, which traps heat and warms the earth's surface (United States Environmental Protection Agency; USEPA, 2019). This warming effect is expected to considerably change the rainfall regimes and increase the frequency of extreme weather events such as flooding, drought, etc. (Harrison et al., 2014). In addition, the increased CO_2 concentration will directly affect crop growth and development (Sreeharsha et al., 2015; Xu et al., 2016), which will further alter food production and agricultural land use (Olesen and Bindi, 2002). The impacts of increasing CO_2 concentration and global warming on extreme climate events, hydrology, and crop production are worldwide concerns (Panagopoulos et al., 2014, 2015; Stefanidis et al., 2018; Ye and Grimm, 2013; Williams et al., 2015). For example, Bourdages and Huard (2010) reported a general increase in temperatures, reduction in the duration of snow period, and increase in most rainfall indicators and extremes under future climate conditions at 12 stations in Ontario, Canada. Using the Soil and Water Assessment Tool (SWAT) model, Chen et al. (2017) simulated that the reductions in crop evapotranspiration (ET) were 12% and 20% for the middle and end of the 21st century, respectively, compared to the historical period (1994–2009) in the Southern High Plains of Texas, U.S. Additionally, Araya et al. (2015) found that simulated increases in CO_2

* Corresponding author.
E-mail address: yongchen@neo.tamu.edu (Y. Chen).

https://doi.org/10.1016/j.agwat.2019.04.021
Received 19 November 2018; Received in revised form 17 April 2019; Accepted 22 April 2019
0378-3774/ © 2019 Elsevier B.V. All rights reserved.

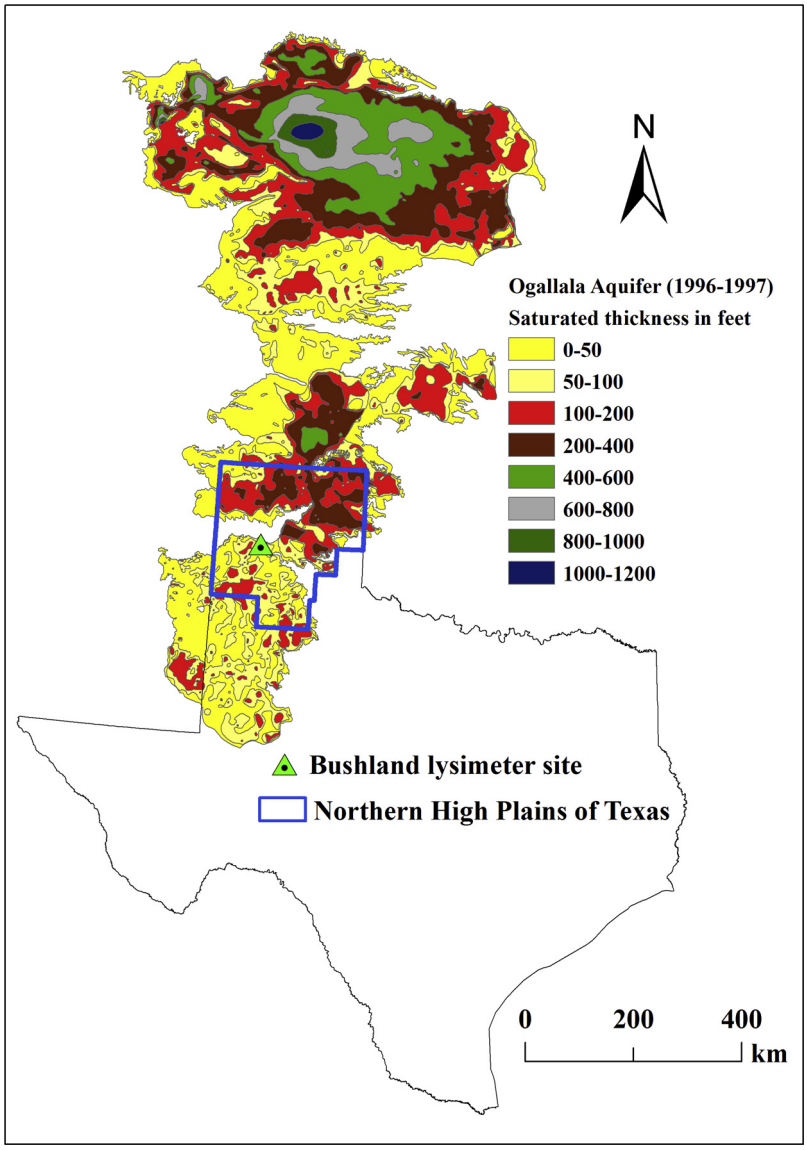

Fig. 1. Locations of the Ogallala Aquifer and the Bushland lysimeter site.

concentrations may contribute to small improvements in corn (*Zea mays* L.) yield during the middle of the 21st century in southwestern Ethiopia using the Decision Support System for Agrotechnology Transfer (DSSAT) and Agricultural Production Systems sIMulator (APSIM) models. However, associated increased air temperatures in the future might have substantial impacts on corn yield reduction.

The semi-arid Northern High Plains (NHP) of Texas is one of the most productive agricultural regions in the U.S. Corn is the dominant irrigated crop grown in the region, and several counties have reported the largest average corn yields in the nation (National Agricultural Statistics Service; NASS, 2019). However, corn is sensitive to water stress and generally requires large amounts of irrigation to supplement inadequate and unreliable rainfall in the NHP. Sorghum (*Sorghum bicolor* L.) is an alternative crop with less sensitivity to water stress and can maintain profitable yields under both irrigated and dryland (rainfed) conditions (Stewart et al., 1983). However, the effects of climate change are complex and uncertain, and vary across regions and time periods. Therefore, it is necessary to explore the potential changes in irrigation water use, ET, and yields of the major crops under future climate scenarios in this region to mitigate any adverse impacts, or to better manage the land use distribution. For instance, most General Circulation Models (GCMs) simulated that the semi-arid NHP would become hotter and drier than usual by the end of this century (Intergovernmental Panel on Climate Change; IPCC, 2007), which might further decrease water availability for crop production in this intensively irrigated agricultural region (Adhikari et al., 2016; Chen et al., 2017; Modala et al., 2017; Seager and Vecchi, 2010). Therefore, the projected future climate may pose challenges to both irrigated and dryland agriculture in this water-limited environment (Barnett et al., 2008; Gober and Kirkwood, 2010).

Some climate change mitigation/adaptation strategies consist of altering crop composition and changing land use regimes (e.g., irrigated farming, dryland farming, and fallow), which show the potential to increase the resilience of agricultural systems to future climate (IPCC, 2001). Changes in land uses from water-intensive crops, such as corn, to less water demanding crops may play a significant role in adapting to climate change (Rose et al., 2012). However, such studies are limited or lack representativeness due to the inadequate simulation of irrigation strategies that use management allowed depletion (MAD) irrigation scheduling, an approach used by producers and researchers in the NHP and in other arid and semi-arid climates around the world (Callison, 2019; Evett et al., 2011; Gheysari et al., 2009; Merriam, 1966; Suarez-Rey et al., 2000). A newly developed automatic irrigation method for simulating MAD-based irrigation scheduling in SWAT (Chen et al.,

2018a) was used in this climate change study to more accurately represent irrigation management in this region. This irrigation algorithm was extensively evaluated across five states in the Southern Great Plains including Texas, Kansas, New Mexico, Colorado, and Nebraska (Chen et al., 2019a), and the results showed the default plant water demand and soil water content automatic irrigation options in SWAT underestimated and overestimated the actual seasonal irrigation, respectively, when compared to the improved MAD automatic irrigation method (Chen et al., 2019a).

The impacts of climate change on hydrology and crop yield were heavily dependent on the types of GCM projections (Bellamy et al., 2002; Williams et al., 2015; Wu et al., 2012a). To better represent the variability of the future climate, projected climate data from 19 GCMs were used in this study. The improved SWAT model equipped with the MAD irrigation scheduling was used in all irrigation simulations. The overall goal of this study was to evaluate the impacts of climate change on the water cycle and crop production under the land uses of corn, sorghum, and fallow in the NHP. Specific objectives of the study were to: (1) quantify the effects of future climate change on hydrologic fluxes and crop yield under corn and sorghum land uses based on 19 GCM projections under two Representative Concentration Pathway (RCP) emission scenarios of RCP 4.5 and RCP 8.5 during four 20-year periods of near future (2020–2039), middle (2040–2059), late (2060–2079), and end (2080–2099) of the 21st century with reference to the respective land use of the historical period (2001–2010) and (2) assess the impacts of long-term continuous fallow on water partitioning under the eight projected future climate change scenarios (2020–2039 RCP 4.5, 2040–2059 RCP 4.5, 2060–2079 RCP 4.5, 2080–2099 RCP 4.5, 2020–2039 RCP 8.5, 2040–2059 RCP 8.5, 2060–2079 RCP 8.5, and 2080–2099 RCP 8.5) compared to the historical period.

2. Materials and methods

2.1. Study area

The study area is located at the U.S. Department of Agriculture-Agricultural Research Service (USDA-ARS) Conservation and Production Research Laboratory (CPRL) at Bushland, Texas (35.2 °N, 102.1 °W, ~1170 m above mean sea level) in the NHP (Fig. 1). The regional climate is classified as semi-arid with an average annual rainfall and temperature of 496 mm and 14.1 °C, respectively. Agricultural production in this region is water limited, with average evaporation exceeding average precipitation in each month (Stewart and Stenier, 1990). The annual standardized alfalfa reference ET (ET_{rs}) is ~1600 mm in the region. The dominant soil is classified as Pullman clay loam (fine, mixed, superactive, thermic Torrertic Paleustoll) (Unger and Pringle, 1981). The major soil characteristics are listed in Table S1. The primary land uses in this study area are irrigated corn, irrigated sorghum, dryland sorghum, and continuous fallow. The Ogallala Aquifer is the source of irrigation for crop production (Fig. 1).

2.2. Improved SWAT model

The SWAT model is a conceptual, physically based, hydrologic model (Arnold et al., 1998). The primary model inputs of topography, soil, land use, climate, and management practices, such as tillage, fertilizer application, irrigation, etc., are required. Recently, Chen et al. (2018a) developed and successfully evaluated an improved automatic irrigation algorithm to simulate MAD-based irrigation scheduling in SWAT. The MAD-based algorithm more accurately simulated typical irrigation practices in the Southern Great Plains region and outperformed the default auto-irrigation functions in comparisons using field measured irrigation data (Chen et al., 2019a). The improved algorithm suspends irrigation after crop harvest and allows for a user-defined depletion of plant available water to trigger irrigations. The MAD algorithm not only links irrigation scheduling to soil water holding properties but also to crop database parameters, such as maximum rooting depth. ArcSWAT 2012 (version 2012.10_2.19; revision 664) equipped with the MAD auto-irrigation algorithm was used for all simulations in this study. The calibrated hydrologic and crop yield parameters for the study area were taken from Chen et al. (2018b). In this study, SWAT simulations for land uses of irrigated corn, irrigated sorghum, dryland sorghum, and continuous fallow during 2000–2010 were used as the historical scenarios (Chen et al., 2018b). The first year (2000) was used to initialize the model. In this study, the "Single HRU method" was used, which means only one hydrologic response unit (HRU) was created to simulate different land uses under climate change scenarios. More details about Single HRU method can be found in Chen et al. (2019b).

2.3. Bias corrections of GCM projections

Climate model data often require bias corrections when projected data are not in agreement with observed data (Figs. S1 and S2) (Christensen et al., 2008; Teutschbein and Seibert, 2010; Varis et al., 2004). Bias corrections use a transformation algorithm to adjust the GCM outputs. The purpose is to identify the possible biases between observed and simulated climate variables, which is the basis for correcting future GCM projections. The bias correction method of distribution mapping is widely used to adjust the GCM projections (Johnson and Sharma, 2011; Rojas et al., 2011; Sennikovs and Bethers, 2009; Sun et al., 2011). The idea of distribution mapping is to correct the distribution function of GCM-simulated climate values to agree with the observed distribution function (Figs. S1 and S2). A transfer function was developed to shift the occurrence distributions of precipitation and temperatures (Sennikovs and Bethers, 2009). This correction approach is also known by several other names found in the literature, including quantile mapping (Boe et al., 2007; Déqué et al., 2007; Johnson and Sharma, 2011; Sun et al., 2011), probability mapping (Block et al., 2009; Ines and Hansen, 2006), statistical downscaling (Piani et al., 2010), and histogram equalization (Rojas et al., 2011; Sennikovs and Bethers, 2009).

Projected daily precipitation, maximum air temperature, and minimum air temperature from 19 GCMs for the 2000–2099 period were obtained from the Downscaled Coupled Model Intercomparison Project Phase 5 (CMIP 5) Climate and Hydrology Projections (http://gdo-dcp.ucllnl.org/) (Reclamation, 2013). GCM climate projections from RCP 4.5 (moderate) and RCP 8.5 (severe) emission scenarios were also considered. RCP refers to radiative forcing pathway that describes an emission concentration by the year 2100 (Van Vuuren et al., 2011). There are four radiative forcing scenarios, which are defined depending on the total radiative forcing in 2100 relative to 1750 (Table S2). RCP 8.5 is a rising scenario with very high greenhouse gas emission of 1350 ppm in 2100 (Riahi et al., 2007). RCPs 4.5 and 6.0 are stabilizing scenarios (Clarke et al., 2007; Fujino et al., 2006; Hijioka et al., 2008; Smith and Wigley, 2006; Wise et al., 2009). RCP 2.6 is a declining scenario with emissions that peak and decline before 2100 (Van Vuuren et al., 2006, 2007). The GCMs used in this study are listed in Table 1. The spatial resolution of the GCM projection is 12.5 km × 12.5 km. The bias correction tool of CMhyd (**C**limate **M**odel data for hydrologic modeling) was used to correct the bias in the downloaded climate data for the study area using the distribution mapping method (Rathjens et al., 2016). The distribution function was used to correct the GCM-simulated climate data for both RCP 4.5 and RCP 8.5 to approximate observed values for the 2000–2010 period. The transfer functions derived from this work were further used to correct the distributions of precipitation and temperatures for the 2020–2099 period of RCP 4.5 and 8.5.

2.4. Scenario development and analysis

Bias-corrected future climate projections from the 19 GCMs were

Table 1
List of the 19 General Circulation Models (GCMs) used in this study.

Model name	Institution/Center	Institute ID	Scenario*
access1-0	Commonwealth Scientific and Industrial Research Organization (CSIRO) and Bureau of Meteorology (BoM), Australia	CSIRO-BoM	RCP 4.5 and 8.5
bcc-csm1-1	Beijing Climate Center, China Meteorological Administration	BCC	RCP 4.5 and 8.5
canesm2	Canadian Centre for Climate Modelling and Analysis	CCCMA	RCP 4.5 and 8.5
ccsm4	National Center for Atmospheric Research	NCAR	RCP 4.5 and 8.5
cesm1-bgc	National Center for Atmospheric Research	NCAR	RCP 4.5 and 8.5
cnrm-cm5	Centre National de Recherches Météorologiques - Centre Européen de Recherche et de Formation Avancée en Calcul Scientifique	CNRM-CERFACS	RCP 4.5 and 8.5
csiro-mk3-6-0	Commonwealth Scientific and Industrial Research Organization in collaboration with Queensland Climate Change Centre of Excellence	CSIRO-QCCCE	RCP 4.5 and 8.5
gfdl-esm2g	NOAA/Geophvsical Fluid Dynamics Laboratory	NOAA GFDL	RCP 4.5 and 8.5
gfdl-esm2m	NOAA/Geophvsical Fluid Dynamics Laboratory	NOAA GFDL	RCP 4.5 and 8.5
inmcm4	Institute of Numerical Mathematics	INM	RCP 4.5 and 8.5
ipsl-cm5a-lr	Institut Pierre Simon Laplace	IPSL	RCP 4.5 and 8.5
ipsl-cm5a-mr	Institut Pierre Simon Laplace	IPSL	RCP 4.5 and 8.5
miroc5	Atmosphere and Ocean Research Institute (The University of Tokyo), National Institute for Environmental Studies, and Japan Agency for Marine-Earth Science and Technology	MIROC	RCP 4.5 and 8.5
miroc-esm	Atmosphere and Ocean Research Institute (The University of Tokyo), National Institute for Environmental Studies, and Japan Agency for Marine-Earth Science and Technology	MIROC	RCP 4.5 and 8.5
miroc-esm-chem	Atmosphere and Ocean Research Institute (The University of Tokyo), National Institute for Environmental Studies, and Japan Agency for Marine-Earth Science and Technology	MIROC	RCP 4.5 and 8.5
mpi-esm-lr	Max Planck Institute for Meteorology (Max-Planck-Institut für Meteorologie)	MPI-M	RCP 4.5 and 8.5
mpi-esm-mr	Max Planck Institute for Meteorology (Max-Planck-Institut für Meteorologie)	MPI-M	RCP 4.5 and 8.5
mri-cgcm3	Meteorological Research Institute	MRI	RCP 4.5 and 8.5
noresm1-m	Norwegian Climate Centre	NCC	RCP 4.5 and 8.5

* RCP: Representative Concentration Pathway.

Table 2
Scenarios of the climate change analysis under corn, sorghum, and fallow land uses.

Time period	Emission scenario*	Assumed average CO_2 concentration (ppm) #
2000-2010	–	330
2020-2039**	RCP 4.5	434
2040-2059	RCP 4.5	485
2060-2079	RCP 4.5	522
2080-2099	RCP 4.5	534
2020-2039	RCP 8.5	448
2040-2059	RCP 8.5	540
2060-2079	RCP 8.5	675
2080-2099	RCP 8.5	841

* RCP: Representative Concentration Pathway.
\# Van Vuuren et al. (2011).
** Five years of data prior to the start of each period were used for the SWAT model warm up (e.g., 2015–2019 is the warm up period for the time period of 2020–2039).

divided into four 20-year periods of 2020–2039 (near future), 2040–2059 (middle of the 21st century), 2060–2079 (late of the 21st century), and 2080–2099 (end of the 21st century). Five years of data prior to the start of each period were used for SWAT model warm up. For example, 2015–2019 was used as the warm up period for the 2020–2039 simulation period. With RCP 4.5 and 8.5 scenarios, the eight future climate change scenarios simulated in this study were 2020–2039 RCP 4.5, 2040–2059 RCP 4.5, 2060–2079 RCP 4.5, 2080–2099 RCP 4.5, 2020–2039 RCP 8.5, 2040–2059 RCP 8.5, 2060–2079 RCP 8.5, and 2080–2099 RCP 8.5. In the SWAT model, atmospheric CO_2 concentration can only be input as a single constant value for a given simulation run. For the historical period (2001–2010), the default SWAT atmospheric CO_2 concentration of 330 ppm was used. According to Van Vuuren et al. (2011), the average CO_2 concentrations for 2020–2039 RCP 4.5, 2040–2059 RCP 4.5, 2060–2079 RCP 4.5, 2080–2099 RCP 4.5, 2020–2039 RCP 8.5, 2040–2059 RCP 8.5, 2060–2079 RCP 8.5, and 2080–2099 RCP 8.5 scenarios were 434, 485, 522, 534, 448, 540, 675, and 841 ppm, respectively (Table 2). Regarding the land uses in the climate change analysis, the irrigated corn, irrigated sorghum, dryland sorghum, and continuous fallow scenarios were considered, and the detailed SWAT management operations of irrigated corn, irrigated sorghum, and dryland sorghum are given in Table 3.

Table 3
Management practices used for irrigated corn, irrigated sorghum, and dryland sorghum in the improved SWAT model.

No.	Management operation	Input data
Irrigated corn (heat units to maturity: 1800 °C-day)		
1	Fertilizer application parameters (May 7)	
	Fertilizer type	Ammonium nitrate
	Fertilizer application rate	644.5 (kg ha^{-1})
2	Planting (Planting on May 14)	Default
3	Irrigation (automatic irrigation) (Start date: May 14; End date: Oct. 19)	
	Water stress identifier	Management allowed depletion
	Depletion threshold of plant available water that triggers irrigation	0.5
4	Harvest and kill (Oct. 19)	Default
Irrigated sorghum (heat units to maturity: 1530 °C-day)		
1	Fertilizer application parameters (May 23)	
	Fertilizer type	Ammonium nitrate
	Fertilizer application rate	612 (kg ha^{-1})
2	Planting (Planting on May 30)	Default
3	Irrigation (automatic irrigation) (Start date: May 30; End date: Oct. 15)	
	Water stress identifier	Management allowed depletion
	Depletion threshold of plant available water that triggers irrigation	0.6
4	Harvest and kill (Oct. 15)	Default
Dryland sorghum (heat units to maturity: 1530 °C-day)		
1	Fertilizer application parameters (June 5)	
	Fertilizer type	Ammonium nitrate
	Fertilizer application rate	170 (kg ha^{-1})
2	Planting (Planting on June 13)	Default
3	Harvest and kill (Oct. 17)	Default

The simulated average annual results for each land use scenario based on projected future climate data by each of the 19 GCMs were averaged for the near future, middle, late, and end of the 21st century and compared with the average (2001–2010) annual historical results for respective land use. Box plots were used to present the percentage or absolute changes between the simulated variables under eight future

Table 4
Simulated precipitation changes (%) for the near future (2020–2039), middle (2040–2059), late (2060–2079), and end (2080–2099) of the 21st century under RCP 4.5 and RCP 8.5 scenarios relative to the historically observed precipitation (2001–2010) of 496 mm.

General circulation model (GCM)	Precipitation RCP 4.5				Precipitation RCP 8.5			
	2020-2039	2040-2059	2060-2079	2080-2099	2020-2039	2040-2059	2060-2079	2080-2099
access1-0	−19.8	−23.3	−21.6	−19.3	−17.2	−10.8	−9.9	−2.8
bcc-csm1-1	−5.0	6.8	10.1	20.0	26.7	0.4	7.6	−9.9
canesm2	−14.1	−19.3	−7.7	−2.9	−12.0	−5.4	3.3	4.5
ccsm4	6.5	−5.9	−5.2	11.6	11.4	13.9	5.5	8.6
cesm1-bgc	−1.2	−29.3	−10.3	−8.7	−23.5	−32.7	−17.8	−29.0
cnrm-cm5	−29.9	−10.5	−22.0	−20.8	3.1	−17.5	−24.0	−3.7
csiro-mk3-6-0	−9.2	9.9	24.5	15.4	−8.3	11.8	−3.7	14.0
gfdl-esm2g	−6.8	−20.9	−6.0	−18.7	−21.9	−9.2	−11.0	−10.8
gfdl-esm2m	7.2	−0.3	19.7	1.3	15.2	12.8	5.3	0.3
inmcm4	9.7	15.6	−2.3	27.5	−1.0	−12.3	−26.6	−19.7
ipsl-cm5a-lr	−11.4	−20.2	−13.4	−5.7	−12.1	−7.6	−17.5	−28.3
ipsl-cm5a-mr	9.4	−11.0	−11.7	12.5	−8.3	−20.6	−40.4	−36.6
miroc5	8.3	10.3	9.3	−9.9	−6.2	17.9	−3.5	−1.3
miroc-esm	53.4	33.6	44.3	37.6	28.1	31.3	50.4	6.1
miroc-esm-chem	−2.0	4.4	17.6	−3.4	7.7	11.7	8.6	20.1
mpi-esm-lr	10.6	8.0	3.9	−9.4	13.1	14.2	−13.3	−12.7
mpi-esm-mr	−26.8	−22.9	−17.4	−26.9	−19.8	6.0	6.4	−3.6
mri-cgcm3	−21.8	−7.7	−13.2	8.3	−6.8	−12.8	−3.3	−9.6
noresm1-m	−21.6	−7.5	−26.5	−12.5	−12.5	−28.9	−16.8	−12.9
Maximum	53.4	33.6	44.3	37.6	28.1	31.3	50.4	20.1
Minimum	−29.9	−29.3	−26.5	−26.9	−23.5	−32.7	−40.4	−36.6
Average	−3.4	−4.8	−1.5	−0.2	−2.3	−2.0	−5.3	−6.7
Median	−5.0	−7.5	−6.0	−3.4	−6.8	−5.4	−3.7	−3.7

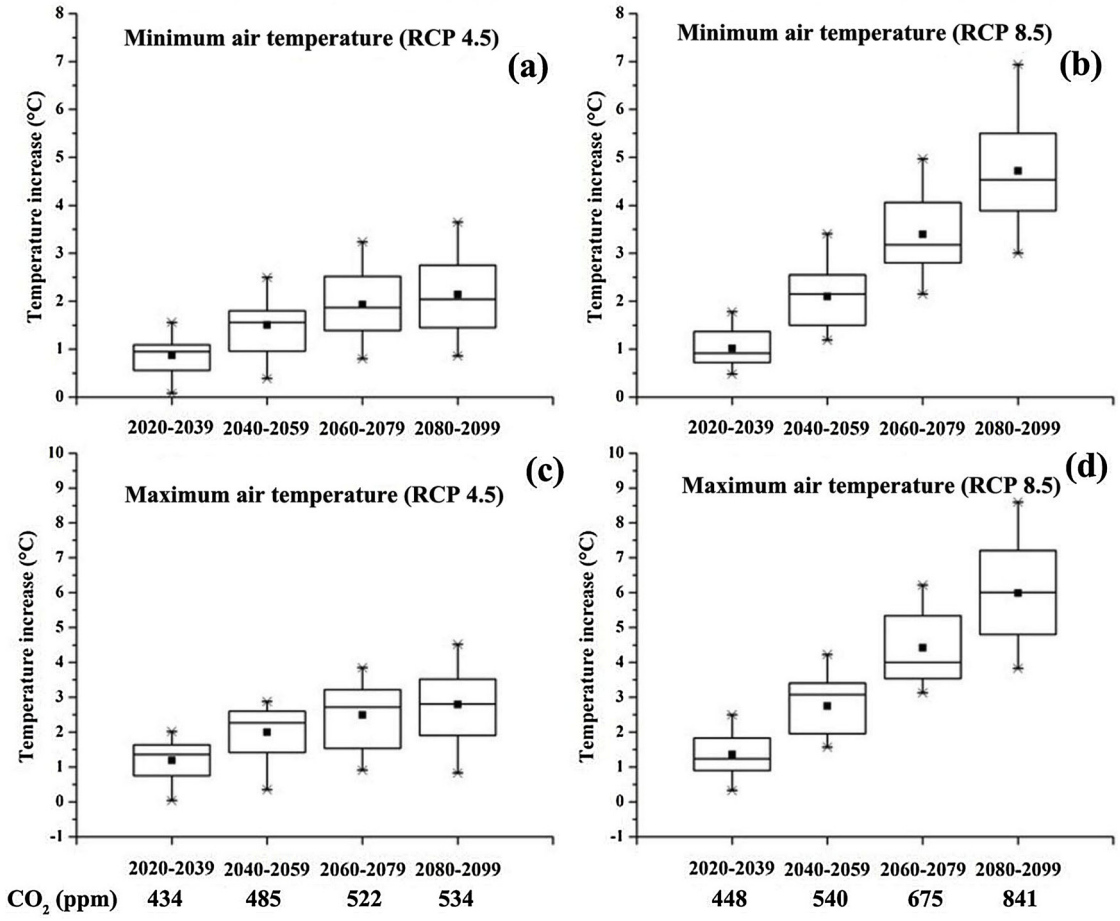

Fig. 2. Box plots showing absolute changes in maximum air temperature and minimum air temperature based on 19 GCM projections under RCP 4.5 and RCP 8.5 scenarios during 2020–2039, 2040–2059, 2060–2079, and 2080–2099 time periods with reference to the historical period (2001–2010).

Table 5
Simulated average annual ET (mm), irrigation (mm), and yield (Mg ha^{-1}) during the historical period (2001–2010) and median annual values of ET, irrigation, and yield under climate change scenarios.

Scenario	Simulated ET	Simulated irrigation	Simulated yield
Irrigated corn land use			
2001–2010	938	450	12.41
2020–2039 RCP 4.5	863 (−7.97*)	382 (−15.09)	12.09 (−2.56)
2040–2059 RCP 4.5	850 (−9.34)	357 (−20.69)	11.70 (−5.71)
2060–2079 RCP 4.5	842 (−10.26)	352 (−21.7)	11.66 (−6.04)
2080–2099 RCP 4.5	834 (−11.1)	352 (−21.7)	11.53 (−7.11)
2020–2039 RCP 8.5	852 (−9.21)	376 (−16.36)	12.08 (−2.68)
2040–2059 RCP 8.5	837 (−10.79)	369 (−17.89)	11.32 (−8.8)
2060–2079 RCP 8.5	800 (−14.75)	308 (−31.62)	10.50 (−15.38)
2080–2099 RCP 8.5	700 (−25.36)	263 (−41.53)	9.67 (−22.04)
Irrigated sorghum land use			
2001–2010	798	305	8.09
2020–2039 RCP 4.5	750 (−5.98)	286 (−6.25)	7.59 (−6.17)
2040–2059 RCP 4.5	729 (−8.68)	266 (−12.92)	6.98 (−13.75)
2060–2079 RCP 4.5	726 (−9.0)	280 (−8.33)	6.70 (−17.16)
2080–2099 RCP 4.5	718 (−10.08)	263 (−13.75)	6.59 (−18.6)
2020–2039 RCP 8.5	745 (−6.58)	294 (−3.75)	7.43 (−8.14)
2040–2059 RCP 8.5	724 (−9.24)	262 (−14.17)	6.58 (−18.7)
2060–2079 RCP 8.5	668 (−16.32)	214 (−30.0)	5.73 (−29.19)
2080–2099 RCP 8.5	580 (−27.29)	155 (−49.17)	4.66 (−42.44)
Dryland sorghum land use			
2001–2010	508	0	2.95
2020–2039 RCP 4.5	445 (−12.48)	0	2.66 (−9.83)
2040–2059 RCP 4.5	455 (−10.39)	0	2.79 (−5.53)
2060–2079 RCP 4.5	448 (11.76)	0	2.76 (−6.44)
2080–2099 RCP 4.5	456 (−10.15)	0	2.95 (0.1)
2020–2039 RCP 8.5	455 (−10.37)	0	2.76 (−6.34)
2040–2059 RCP 8.5	441 (−13.15)	0	2.76 (−6.34)
2060–2079 RCP 8.5	438 (−13.79)	0	2.87 (−2.68)
2080–2099 RCP 8.5	427 (−15.85)	0	2.79 (−5.46)
Fallow land use		0	
2001–2010	457	0	0
2020–2039 RCP 4.5	371 (−18.75)	0	0
2040–2059 RCP 4.5	383 (−16.16)	0	0
2060–2079 RCP 4.5	380 (−16.75)	0	0
2080–2099 RCP 4.5	391 (−14.49)	0	0
2020–2039 RCP 8.5	382 (−16.36)	0	0
2040–2059 RCP 8.5	366 (−19.98)	0	0
2060–2079 RCP 8.5	367 (−19.61)	0	0
2080–2099 RCP 8.5	352 (−22.97)	0	0

* The number in the parentheses is the percent change of each climate change scenario relative to the respective land use during the historical period.

climate change scenarios and the historical period.

3. Results and discussion

3.1. Simulated future climate of the study area

The median annual precipitation projected by 19 GCMs was decreased by 3%–8% under eight future climate change scenarios when compared to the precipitation during the historical period (2001–2010) (Table 4). However, a high degree of uncertainty existed in projected annual precipitation. For example, 12 GCMs simulated a decrease in the annual precipitation with a range of 3% to 40%, while 7 GCMs projected an increase in the precipitation by 3% to 50% under the 2060–2079 RCP 8.5 scenario relative to the historical precipitation (Table 4). It is interesting to note that the precipitation during the growing season (May to October) was increased by 0.5%–3.6% under the RCP 4.5 scenario (Fig. S3) and changed from -1.2% to 2.2% under the RCP 8.5 scenario (Fig. S4). Generally, the future precipitation is favorable to the summer crop production. Increasing CO_2 concentration in the future will trap heat, and hence warm the earth surface, which is expected to further influence the precipitation distribution (USEPA, 2019).

The median annual minimum air temperature increased by 1.0°C, 1.6°C, 1.9°C, 2.0°C, 0.9°C, 2.2°C, 3.2°C, and 4.5°C under the 2020–2039 RCP 4.5, 2040–2059 RCP 4.5, 2060–2079 RCP 4.5, 2080–2099 RCP 4.5, 2020–2039 RCP 8.5, 2040–2059 RCP 8.5, 2060–2079 RCP 8.5, and 2080–2099 RCP 8.5 scenarios, respectively, compared to the historical minimum air temperature (Fig. 2a, b). The increase in median minimum air temperature during the growing season was even larger with the corresponding values of 1.1, 2.0, 2.3, 2.5, 1.4, 3.2, 4.7, and 6.1°C (Figs. S5 and S6). The median annual maximum air temperature also increased by 1.4°C, 2.3°C, 2.7°C, and 2.8°C under the RCP 4.5 scenarios of 2020–2039, 2040–2059, 2060–2079, and 2080–2099, respectively, relative to the historical maximum air temperature (Fig. 2c). Those increases were 1.2°C, 3.1°C, 4.0°C, and 6.0°C under the RCP 8.5 scenarios of 2020–2039, 2040–2059, 2060–2079, and 2080–2099, respectively (Fig. 2d). A slightly higher increase in median maximum air temperature during growing season was predicted compared to the annual increase value, which varied from 1.4 to 3.0°C and 1.4 to 6.1°C under the RCP 4.5 and 8.5 scenarios, respectively (Figs. S7 and S8).

The increases in temperatures were evident in the late and end of the 21st century with the highest increase for the 2080–2099 RCP 8.5 scenario, which also had the highest estimated CO_2 concentration (841 ppm) (Fig. 2d; Table 2). In general, the severe emission scenario (RCP 8.5) had higher temperature increase level compared to the moderate emission scenario (RCP 4.5). Prolonged periods of high temperatures in the Texas High Plains have previously caused severe drought events in 2011 and 2012 (Claeys and Inzé, 2013; Hoerling et al., 2013). Shafer et al. (2014) also predicted that large parts of Texas will experience longer droughts, with the number of consecutive dry days increasing by up to 5 days by 2065. However, when rainfall occurs, it is likely to be more intense, with a 10%–15% increase in maximum 1-day precipitation amount.

3.2. Climate change impact on irrigated corn

The simulated average annual crop ET, irrigation, and yield during the historical period (2001–2010) was reported in Table 5 (Chen et al., 2018b). The simulated median annual ET of irrigated corn based on the 19 GCM projections decreased by 8.0%, 9.3%, 10.3%, 11.1%, 9.2%, 10.8%, 14.8%, and 25.4% under the 2020–2039 RCP 4.5, 2040–2059 RCP 4.5, 2060–2079 RCP 4.5, 2080–2099 RCP 4.5, 2020–2039 RCP 8.5, 2040–2059 RCP 8.5, 2060–2079 RCP 8.5, and 2080–2099 RCP 8.5 scenarios, respectively, compared to the historical corn ET (Fig. 3a, b). In addition, all GCMs simulated the reduction trends of ET under eight climate change scenarios. The elevated CO_2 concentration from the historical period of 330 ppm to 434–841 ppm of various future climate scenarios was the dominant factor for the reduction in the simulated ET for corn in this study region. Crop stomatal apertures will close partially to hinder transpiration in response to increased CO_2 concentration (Leakey et al., 2009; Sreeharsha et al., 2015; Xu et al., 2016), and the SWAT model is able to represent this crop response (Butcher et al., 2014; Wu et al., 2012b). The decline in the future median annual corn ET resulted in reductions in the median annual irrigation water use (Ficklin et al., 2009). The median annual irrigation water use for future corn production was reduced by 15.1%, 20.7%, 21.7%, 21.7%, 16.4%, 17.9%, 31.6%, and 41.5% under the 2020–2039 RCP 4.5, 2040–2059 RCP 4.5, 2060–2079 RCP 4.5, 2080–2099 RCP 4.5, 2020–2039 RCP 8.5, 2040–2059 RCP 8.5, 2060–2079 RCP 8.5, and 2080–2099 RCP 8.5 scenarios, respectively, compared to the historical corn irrigation amount (Fig. 3c, d). The decrease in the future corn irrigation was the highest under the 2080–2099 RCP 8.5 scenario with the highest CO_2 projection as compared to other future climate scenarios.

The simulated median irrigated corn yield decreased under all eight climate change scenarios. These reductions were relatively smaller and varied from 2.6%–7.1% under the RCP 4.5 scenarios for 2020–2039, 2040–2059, 2060–2079, and 2080–2099 periods, relative to corn yield

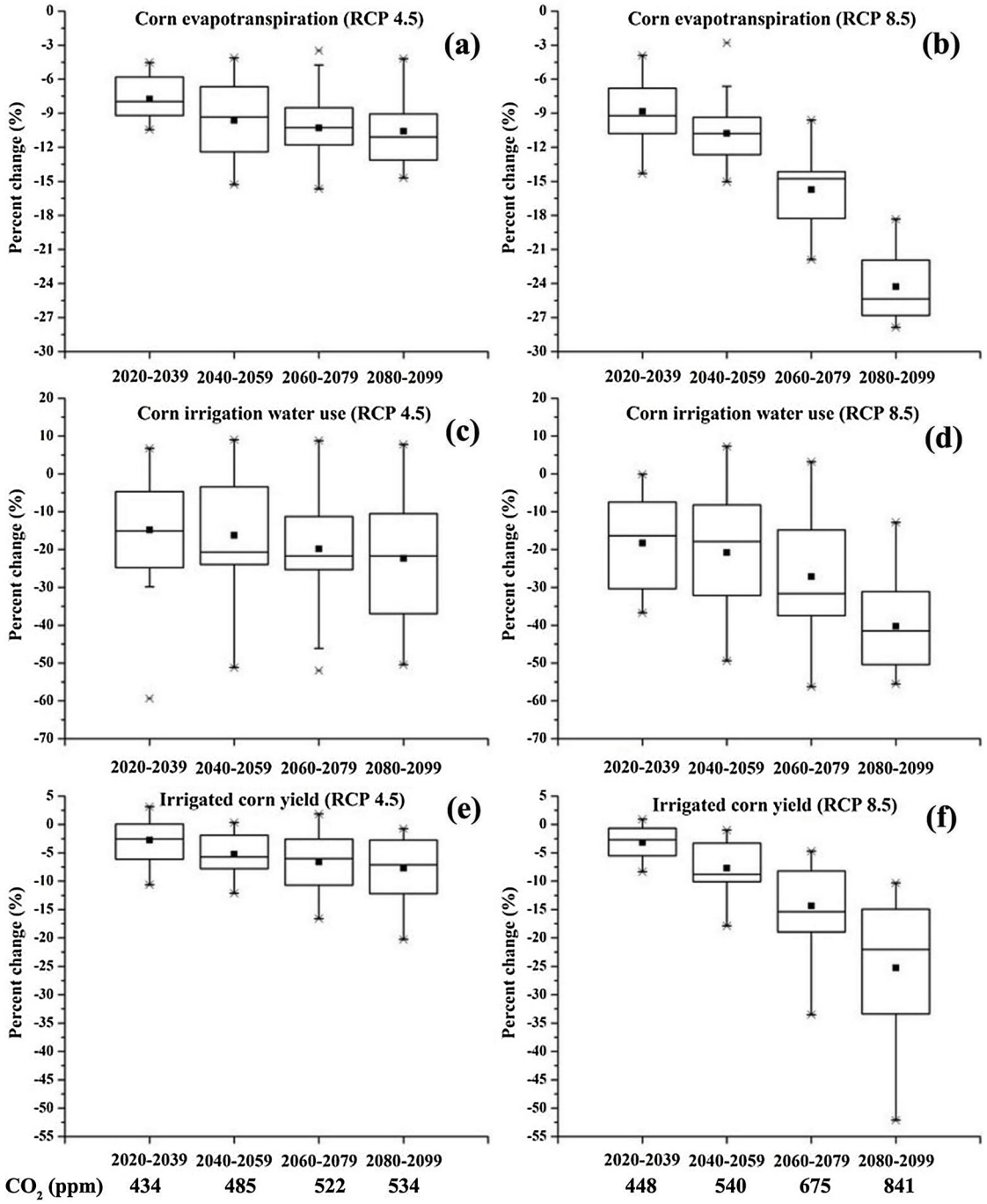

Fig. 3. Box plots showing average annual percent changes in actual corn evapotranspiration, corn irrigation water use, and corn yield based on 19 GCM projections under RCP 4.5 and RCP 8.5 scenarios during 2020–2039, 2040–2059, 2060–2079, and 2080–2099 time periods compared to the baseline corn scenario over the historical period (2001–2010).

for the historical period (Fig. 3e). However, median irrigated corn yield decreased exponentially for the latter half of the 21st century under RCP 8.5 scenarios with yield varying from 8.8%–22.0% (Fig. 3f). Cotterman et al. (2018) also found that the simulated irrigated corn yields were relatively insensitive to the projected climate change scenarios for the first half of the 21st century (through 2050) in the Central High Plains, U.S. However, the simulated irrigated corn yields showed a more pronounced decline towards the end of the century under RCP 8.5 scenario. Wang et al. (2017) also simulated decreases in corn yields by 6% in the 2021–2050 period and 16% reductions in the 2061–2090 period in the St. Joseph River watershed in the Eastern U.S. Corn Belt using SWAT. The decrease in projected irrigated corn yield was mainly attributed to the shortening of the maturity period, which was caused by the increase of future temperatures in the study area. Reduced maturity period could decrease time duration of corn to use solar radiation and assimilate CO_2, which adversely influences the accumulation of corn biomass and final yield (Araya et al., 2017; Cotterman et al., 2018; Islama et al., 2012; Bassu et al., 2014).

3.3. Climate change impact on irrigated sorghum

The simulated median annual ET reductions of irrigated sorghum ranged from 6.0% to 10.1% (Fig. 4a) and 6.6% to 27.3% (Fig. 4b) under RCP 4.5 and RCP 8.5 scenarios, respectively, compared to the

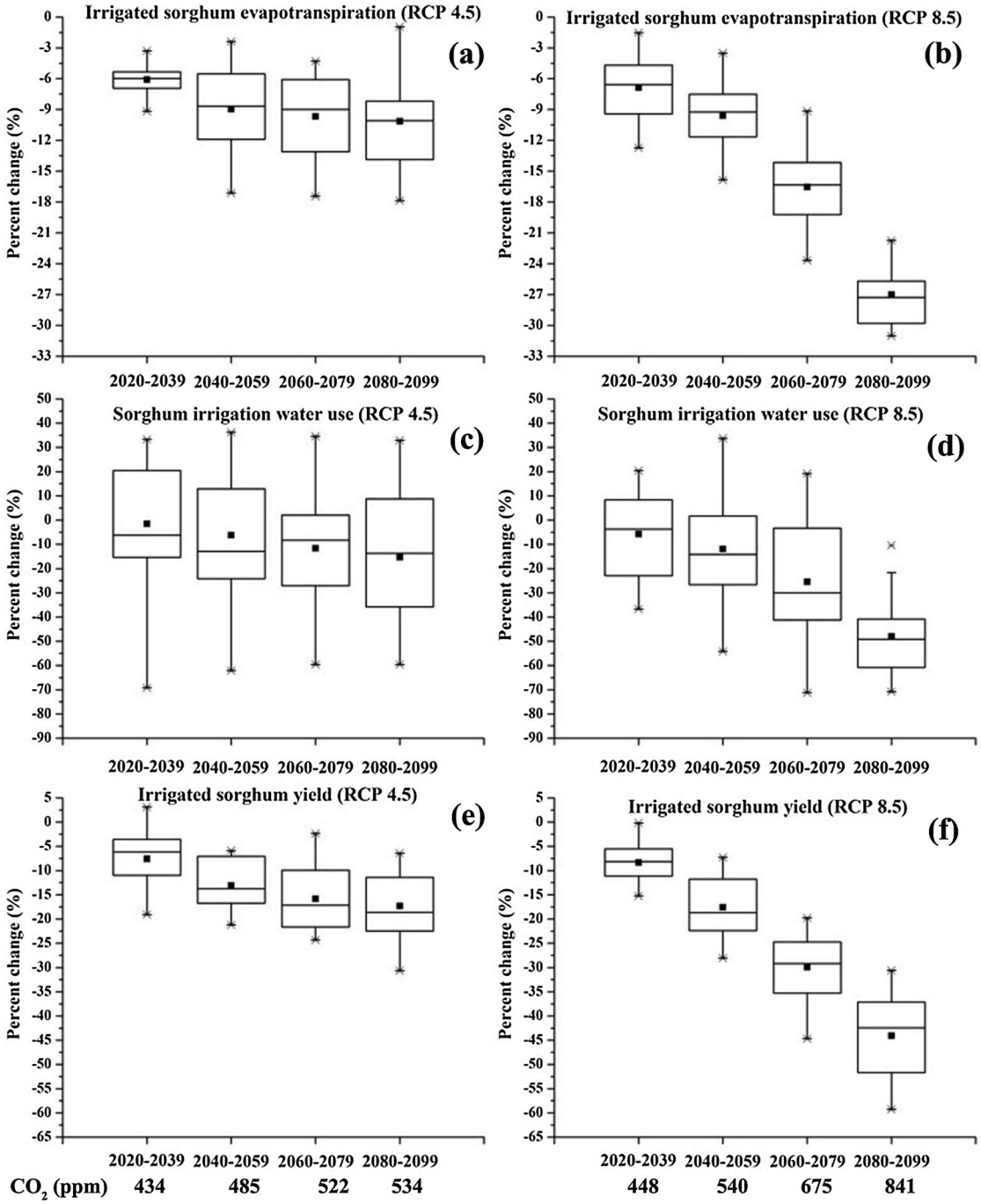

Fig. 4. Box plots showing average annual percent changes in actual sorghum evapotranspiration, sorghum irrigation water use, and sorghum yield based on 19 GCM projections under RCP 4.5 and RCP 8.5 scenarios during 2020–2039, 2040–2059, 2060–2079, and 2080–2099 time periods compared to the baseline sorghum scenario over the historical period (2001–2010).

historically irrigated sorghum ET. Similar to irrigated corn, SWAT simulated ET reductions for all four periods and emissions scenarios due to the projected increase in CO_2 concentrations. However, the decline in the median annual irrigation water use of sorghum was within 15% relative to the historical irrigation amount, except for the 2060–2079 and 2080–2099 periods under RCP 8.5 scenarios with 30.0% and 49.2% reductions in median annual irrigation (Fig. 4c, d). A large variation in the simulated future irrigation for sorghum by 19 GCMs was found, which was primarily due to the relatively small seasonal irrigation amount of sorghum under the historical period (305 mm) compared to the historical precipitation amount of 496 mm. Therefore, the considerable variation of the future precipitation may greatly affect future irrigation water use of the less water demanding sorghum production.

A decline in irrigated sorghum yield was simulated for nearly all the GCM projections of the eight climate change scenarios when compared to the historical sorghum scenario (Fig. 4e, f). Similar to corn, the major reason for the decline in the irrigated sorghum yield was the global warming effect and the associated early crop maturity in the study region. Sorghum requires ˜15% fewer heat units than corn to reach physiological maturity. Therefore, the increase of temperatures led to reductions of irrigated sorghum yields that ranged from 6.2% to 18.6% and 8.1% to 42.4% under the RCP 4.5 and 8.5 scenarios, respectively. Overall, in view of the irrigated land uses, future climate should play a key role in water saving. However, climate change will also present

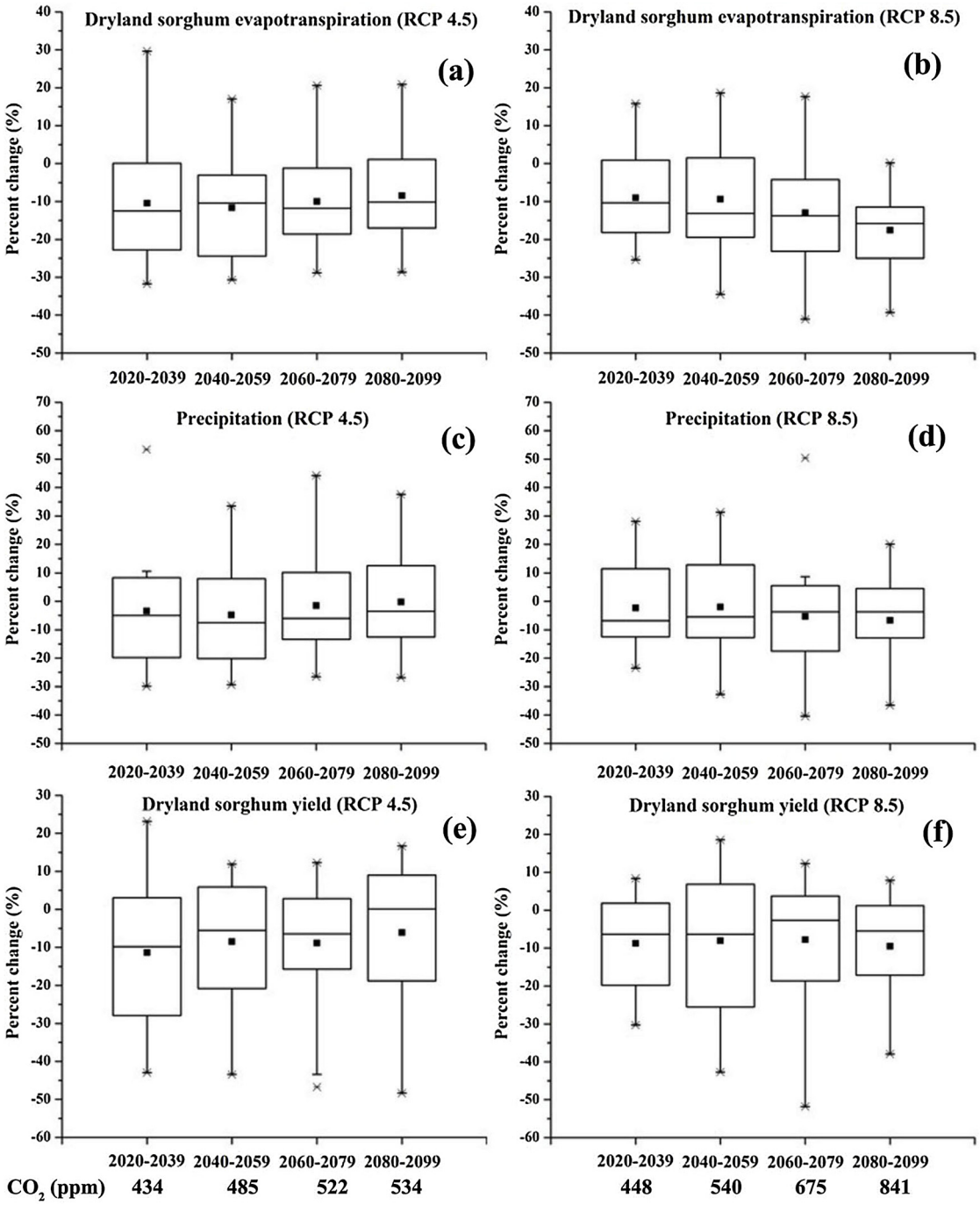

Fig. 5. Box plots showing average annual percent changes in dryland sorghum actual evapotranspiration, precipitation, and dryland sorghum yield based on 19 GCM projections under RCP 4.5 and RCP 8.5 scenarios during 2020–2039, 2040–2059, 2060–2079, and 2080–2099 time periods with reference to the historical period (2001–2010).

additional risks and challenges for crop production and food security.

3.4. Climate change impact on dryland sorghum and continuous fallow

The decrease in simulated median annual ET ranged from 10% to 16% for the eight climate change scenarios compared to the historical dryland sorghum ET (Fig. 5a, b). Under dryland conditions in the semi-arid NHP region, projected reduction in precipitation can have a crucial role in the water cycle and crop production (Fig. 5c, d). The reduction in dryland sorghum median yield was within 10% of the historical dryland sorghum yield (Fig. 5e, f). Similar to the changes in projected precipitation, simulated future dryland sorghum ET and yield displayed decreased trends but with high uncertainties. Using the DSSAT model, Kothari et al. (2017) also reported a reduction in irrigated sorghum yield by 6% and 8%, and a decrease in dryland sorghum yield by 9% and 17% under future climate for the 2040–2070 period under RCP 4.5 and 8.5 scenarios, respectively, compared to the historical period (1980–2010) at Helms Farm near Halfway in the Texas High Plains.

As for the continuous fallow land use, the future median annual evaporation decreased by 18.8%, 16.2%, 16.8%, 14.5%, 16.4%, 20.0%, 19.6%, and 23.0% under the 2020–2039 RCP 4.5, 2040–2059 RCP 4.5, 2060–2079 RCP 4.5, 2080–2099 RCP 4.5, 2020–2039 RCP 8.5, 2040–2059 RCP 8.5, 2060–2079 RCP 8.5, and 2080–2099 RCP 8.5 scenarios, respectively, compared to the historical evaporation of the

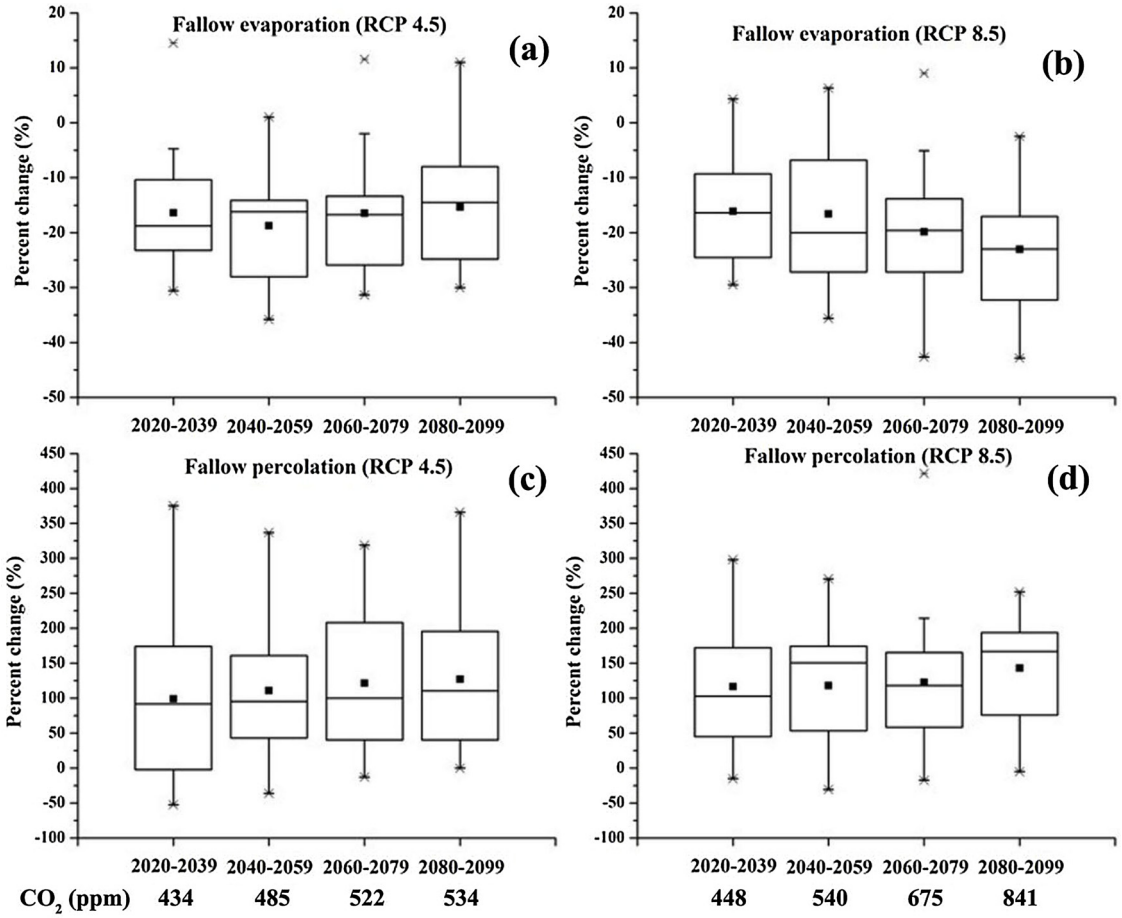

Fig. 6. Box plots showing average annual percent changes in fallow evaporation and percolation based on 19 GCM projections under RCP 4.5 and RCP 8.5 scenarios during 2020–2039, 2040–2059, 2060–2079, and 2080–2099 time periods with reference to the historical period (2001–2010).

fallow land use (Fig. 6a, b). The reduction in median annual precipitation amount and the shift of precipitation distribution could be the dominant factors for the decreased future median annual evaporation in this region. Regarding percolation/groundwater recharge, the simulated median annual percolation increased by 91.9%, 95.4%, 100.2%, 110.6%, 102.9%, 150.9%, 118.2%, and 167.2% under the corresponding climate change scenarios (Fig. 6c, d). The large increase in the simulated future percolation also emphasized that there was an increase in the precipitation duration projected by the GCMs. Zhang et al. (2017) and others suggested that fallow is a possible adaptation strategy for the climate change, where the agricultural land is left idle to accumulate soil moisture and recharge groundwater as a means of adapting to future dry conditions (Bradshaw et al., 2004; Howden et al., 2007; Verchot et al., 2007). Their climate change study also found future climate caused producers to shift cropland into fallow to deal with the decrease in future precipitation in the U.S. Pacific Northwest. Moreover, according to a five-year field experiment (2007–2012) in Garden City, Kansas, Holman et al. (2018) also recommended that the fallow period was beneficial for dryland winter wheat production. Therefore, the occasional fallow may not only increase groundwater recharge but also enhance dryland crop production for the following year.

4. Conclusions

An improved SWAT model assembled with a MAD automatic irrigation function was used to explore the impacts of climate change on hydrology and crop production of irrigated corn, irrigated sorghum, dryland sorghum, and continuous fallow land uses in the NHP. Bias-corrected climate data using a distribution mapping method for four 20-year periods of near future (2020 to 2039), middle (2040 to 2059), late (2060 to 2079), and end (2080 to 2099) of the 21st century under RCP 4.5 and 8.5 scenarios according to 19 GCM projections were investigated in this study. The future climate data projected that temperatures will increase significantly, particularly during the crop growing season (May to October). The future annual precipitation will decrease by 3%–8% and mainly in months of January and February. The SWAT simulated results showed that median annual ET and irrigation of corn land use was reduced by 8%–25% and 15%–42%, respectively, under the future climate change scenarios when compared to the historical period (2001–2010). Low crop stomatal conductance due to elevated CO_2 concentration inhibited transpiration, and hence reduced plant ET. The median annual ET and irrigation reductions of irrigated sorghum ranged from 6% to 27% and 4% to 49%, respectively. The decrease in simulated median annual ET ranged from 10% to 16% compared to the historical dryland sorghum ET. The future median annual evaporation decreased by 15%–23% for the continuous fallow land use. However, a considerable increase in the median annual percolation by 92%–167% was predicted.

The median irrigated corn and sorghum yields decreased by 3%–22% and 6%–42% relative to the historically irrigated corn and sorghum yields, which mainly caused by the increase in temperatures and the associated curtailment of the maturity period. However, the reduction in dryland sorghum median yield was within 10% compared to the historical dryland sorghum yield. The results from this study denoted that the historical or current climate was more appropriate for the irrigated sorghum production with less irrigation use and profitable yield. However, the irrigated corn showed less yield reduction potential

and more irrigation water saving compared to the irrigated sorghum under the future climate. Under dryland conditions, projected future precipitation will directly influence the water cycle and crop growth. In general, an increased amount of precipitation will become percolation and surface runoff rather than ET for the future dryland land uses. However, the projected future climate is complex and uncertain. This study provided an overview of the impact of climate change on the water use and crop production under different land uses in the NHP to sustain the identification and development of climate adaptation strategies at local to regional scales.

Acknowledgments

This research was supported in part by the Ogallala Aquifer Program, a consortium between USDA-Agricultural Research Service, Kansas State University, Texas A&M AgriLife Research, Texas A&M AgriLife Extension Service, Texas Tech University, and West Texas A&M University. We acknowledge the modeling groups, the Program for Climate Model Diagnosis and Intercomparison (PCMDI) and the World Climate Research Programme's (WCRP's) Working Group on Coupled Modelling (WGCM) for their roles in making available the WCRP CMIP3 and CMIP5 multi-model dataset. Support of this dataset is provided by the Office of Science, U.S. Department of Energy.

Appendix A. Supplementary data

Supplementary material related to this article can be found, in the online version, at doi:https://doi.org/10.1016/j.agwat.2019.04.021.

References

Adhikari, P., Ale, S., Bordovsky, J.P., Thorp, K.R., Modala, N.R., Rajan, N., Barnes, E.M., 2016. Simulating future climate change impacts on seed cotton yield in the Texas High Plains using the CSM-CROPGRO-Cotton model. Agric. Water Manage. 164, 317–330.

Araya, A., Hoogenboom, G., Luedeling, E., Hadgu, K.M., Kisekka, I., Martorano, L.G., 2015. Assessment of maize growth and yield using crop models under present and future climate in southwestern Ethiopia. Agric. For. Meteorol. 214–215, 252–265.

Araya, A., Kisekka, I., Lin, X., Prasad, P.V., Gowda, P.H., Rice, C., Andales, A., 2017. Evaluating the impact of future climate change on irrigated maize production in Kansas. Clim. Risk Manage. 17, 139–154.

Arnold, J.G., Srinivasan, R., Muttiah, R.S., Williams, J.R., 1998. Large-area hydrologic modeling and assessment: part I. Model development. J. Am. Water Resour. Assoc. 34, 73–89.

Barnett, T.P., Pierce, D.W., Hidalgo, H.G., Bonfils, C., Santer, B.D., Das, T., Bala, G., Wood, A.W., Nozawa, T., Mirin, A.A., Cayan, D.R., Dettinger, M.D., 2008. Human-induced changes in the hydrology of the Western United States. Science 319, 1080–1083.

Bassu, S., Brisson, N., Durand, J.L., Boote, K., Lizaso, J., Jones, J.W., Rosenzweig, C., Ruane, A.C., Adam, M., Baron, C., Basso, B., 2014. How do various maize crop models vary in their responses to climate change factors? Glob. Change Biol. 20 (7), 2301–2320.

Bellamy, S., Boyd, D., Minshall, L., 2002. Determining the Effect of Climate Change on the Hydrology of the Grand River Watershed. Grand River Conservation Authority, Cambridge.

Block, P.J., Souza Filho, F.A., Sun, L., Kwon, H.H., 2009. A streamflow forecasting framework using multiple climate and hydrological models. J. Am. Water Resour. As. 45 (4), 828–843.

Boe, J., Terray, L., Habets, F., Martin, E., 2007. Statistical and dynamical downscaling of the Seine basin climate for hydro-meteorological studies. Int. J. Climatol. 27 (12), 1643–1655.

Bourdages, L., Huard, D., 2010. Climate Change Scenario Over Ontario Based on the Canadian Regional Climate Model (CRCM4.2). Ouranos, Montreal, Quebec, Canada.

Bradshaw, B., Dolan, H., Smit, B., 2004. Farm-level adaptation to climate variability and change: crop diversification in the Canadian Prairies. Clim. Change 67 (1), 119–141.

Butcher, J.B., Johnson, T.E., Nover, D., Sarkar, S., 2014. Incorporating the effects of increased atmospheric CO_2 in watershed model projections of climate change impacts. J. Hydrol. 513, 322–334.

Callison, D., 2019. Management Allowed Depletion Irrigation Scheduling. Available online: http://awqa.org/wp-content/toolkits/IrrigationScheduling/ManagementAllowedDepletion-IrrigationScheduling.pdf (Accessed on 3 October 2018). .

Chen, Y., Ale, S., Rajan, N., Srinivasan, R., 2017. Modeling the effects of land use change from cotton (*Gossypium hirsutum* L.) to perennial bioenergy grasses on watershed hydrology and water quality under changing climate. Agric. Water Manage. 192, 198–208.

Chen, Y., Marek, G.W., Marek, T.H., Brauer, D.K., Srinivasan, R., 2018a. Improving SWAT auto-irrigation functions for simulating agricultural irrigation management using long-term lysimeter field data. Environ. Model. Softw. 99, 25–38.

Chen, Y., Marek, G.W., Marek, T.H., Moorhead, J.E., Heflin, K.R., Brauer, D.K., Gowda, P.H., Srinivasan, R., 2018b. Assessment of alternative agricultural land use options for extending the availability of the Ogallala Aquifer in the Northern High Plains of Texas. Hydrology 5 (4), 53.

Chen, Y., Marek, G.W., Marek, T.H., Gowda, P.H., Xue, Q., Moorhead, J.E., Brauer, D.K., Srinivasan, R., Heflin, K.R., 2019a. Multisite evaluation of an improved SWAT irrigation scheduling algorithm for the Southern Great Plains. Environ. Model. Softw. 118, 23–34.

Chen, Y., Marek, G.W., Marek, T.H., Xue, Q., Brauer, D.K., Srinivasan, R., 2019b. Assessing Soil and Water Assessment Tool plant stress algorithms using full and deficit irrigation treatments. Agron. J. 111, 1–15.

Christensen, J.H., Boberg, F., Christensen, O.B., Lucas-Picher, P., 2008. On the need for bias correction of regional climate change projections of temperature and precipitation. Geophys. Res. Lett. 35 (20), L20709.

Claeys, H., Inzé, D., 2013. The agony of choice: how plants balance growth and survival under water-limiting conditions. Plant Physiol. 162, 1768–1779.

Clarke, L.E., Edmonds, J.A., Jacoby, H.D., Pitcher, H., Reilly, J.M., Richels, R., 2007. Scenarios of Greenhouse Gas Emissions and Atmospheric Concentrations. Sub-report 2.1A of Synthesis and Assessment Product 2.1. Climate Change Science Program and the Subcommittee on Global Change Research, Washington DC.

Cotterman, K.A., Kendall, A.D., Basso, B., Hyndman, D.W., 2018. Groundwater depletion and climate change: future prospects of crop production in the Central High Plains Aquifer. Clim. Change 146 (1-2), 187–200.

Déqué, M., Rowell, D.P., Lüthi, D., Giorgi, F., Christensen, J.H., Rockel, B., Jacob, D., Kjellström, E., De Castro, M., van den Hurk, B., 2007. An intercomparison of regional climate simulations for Europe: assessing uncertainties in model projections. Clim. Change 81, 53–70.

Evett, S.R., Schwartz, R.C., Mazahrih, N.T., Jitan, M.A., Shaqir, I.M., 2011. Soil water sensors for irrigation scheduling: Can they deliver a management allowed depletion? Acta Hortic. 888, 231–237.

Ficklin, D.L., Luo, Y.Z., Luedeling, E., Zhang, M.H., 2009. Climate change sensitivity assessment of a highly agricultural watershed using SWAT. J. Hydrol. 374, 16–29.

Fujino, J., Nair, R., Kainuma, M., Masui, T., Matsuoka, Y., 2006. Multi-gas mitigation analysis on stabilization scenarios using AIM global model. Energy J. 27, 343–354.

Gheysari, M., Mirlatifi, S.M., Homaee, M., Asadi, M.E., Hoogenboom, G., 2009. Nitrate leaching in a silage maize field under different irrigation and nitrogen fertilizer rates. Agric. Water Manage. 96, 946–954.

Gober, P., Kirkwood, C.W., 2010. Vulnerability assessment of climate-induced water shortage in Phoenix. Proc. Natl. Acad. Sci. 107 (50), 21295–21299.

Harrison, M., Tardieu, F.O., Dong, Z., Messina, C.D., Hammer, G., 2014. Characterizing drought stress and trait influence on maize yield under current and future conditions. Glob. Change Biol. 20 (3), 867–878.

Hijioka, Y., Matsuoka, Y., Nishimoto, H., Masui, T., Kainuma, M., 2008. Global GHG emission scenarios under GHG concentration stabilization targets. J. Glob. Environ. Eng. 1, 97–108.

Hoerling, M., Kumar, A., Dole, R., Nielsen-Gammon, J.W., Eischeid, J., Perlwitz, J., Quan, X.W., Zhang, T., Pegion, P., Chen, M., 2013. Anatomy of an extreme event. J. Clim. 26 (9), 2811–2832.

Holman, J.D., Arnet, K., Dille, J., Maxwell, S., Obour, A., Roberts, T., Roozeboom, K., Schlegel, A., 2018. Can cover or forage crops replace fallow in the semiarid Central Great Plains? Crop Sci. 58, 932–944.

Howden, S.M., Soussana, J., Tubiello, F.N., Chhetri, N., Dunlop, M., Meinke, H., 2007. Adapting agricultural to climate change. Proc. Natl. Acad. Sci. 104 (50), 19691–19696.

Ines, A.V.M., Hansen, J.W., 2006. Bias correction of daily GCM rainfall for crop simulation studies. Agric. For. Meteorol. 138 (1-4), 44–53.

Intergovernmental Panel on Climate Change (IPCC), 2001. Climate Change 2001: Impacts, Adaptation, and Vulnerability Contribution of Working Group II to the Third Assessment Report of the Intergovernmental Panel on Climate Change. Cambridge University Press, Cambridge, United Kingdom and New York, NY, USA.

Intergovernmental Panel on Climate Change (IPCC), 2007. Climate Change 2007: The Physical Science Basis. Contribution of Working Group I to the Fourth Assessment Report of the Intergovernmental Panel on Climate Change. Cambridge University Press, Cambridge, United Kingdom and New York, NY, USA.

Islama, A., Ahuja, R.L., Garciab, L.A., Ma, L., Saseendran, A.S., Trout, T.J., 2012. Modeling the impacts of climate change on irrigated maize production in the Central Great Plains. Agric. Water Manage. 110, 94–108.

Johnson, F., Sharma, A., 2011. Accounting for interannual variability: a comparison of options for water resources climate change impact assessments. Water Resour. Res. 47 (4), W04508.

Kothari, K., Ale, S., Bordovsky, J., Hoogenboom, G., Munster, C.L., 2017. Assessment of climate change impacts and evaluation of adaptation strategies for grain sorghum and cotton production in the Texas High plains. AGU Fall Meeting Abstracts. . December Available online: http://adsabs.harvard.edu/abs/2017AGUFMGC41D1044K (Accessed on 10 October 2018).

Leakey, A.D., Ainsworth, E.A., Bernacchi, C.J., Rogers, A., Long, S.P., Ort, D.R., 2009. Elevated CO_2 effects on plant carbon, nitrogen, and water relations: six important lessons from FACE. J. Exp. Bot. 60 (10), 2859–2876.

Merriam, J.L., 1966. A management control concept for determining the economical depth and frequency of irrigation. Trans. ASAE 9 (4), 492–498.

Modala, N.R., Ale, S., Goldberg, D., Olivares, M., Munster, C., Rajan, N., Feagin, R., 2017. Climate change projections for the Texas High Plains and Rolling Plains. Theor. Appl. Climatol. 129 (1), 263–280.

National Agricultural Statistics Service (NASS), 2019. National Agricultural Statistics Service (NASS). Available online: https://www.nass.usda.gov/ (Accessed on 17 October 2018). .

Olesen, J.E., Bindi, M., 2002. Consequences of climate change for European agricultural productivity, land use and policy. Eur. J. Agron. 16 (4), 239–262.

Panagopoulos, Y., Gassman, P.W., Arritt, R.W., Herzmann, D.E., Campbell, T.D., Jha, M.K., Kling, C.L., Srinivasan, R., White, M., Arnold, J.G., 2014. Surface water quality and cropping systems sustainability under a changing climate in the Upper Mississippi River Basin. J. Soil Water Conserv. 69 (6), 483–494.

Panagopoulos, Y., Gassman, P.W., Arritt, R.W., Herzmann, D.E., Campbell, T.D., Valcu, A., Jha, M.K., Kling, C.L., Srinivasan, R., White, M., Arnold, J.G., 2015. Impacts of climate change on hydrology, water quality and crop productivity in the Ohio-Tennessee River Basin. Int. J. Agric. Biol. Eng. 8 (3), 36–53.

Downscaled CMIP3 and CMIP5 Climate Projections: Release of Downscaled CMIP5 Climate Projections, Comparison with Preceding Information, and Summary of User Needs. U.S. Department of the Interior, Bureau of Reclamation, 104 p., Available at: http://gdo-dcp.ucllnl.org/downscaled_cmip_projections/techmemo/downscaled_ climate.pdf (Accessed on 28 April 2019).

Piani, C., Haerter, J.O., Coppola, E., 2010. Statistical bias correction for daily precipitation in regional climate models over Europe. Theor. Appl. Climatol. 99 (1), 187–192.

Rathjens, H., Bieger, K., Srinivasan, R., Chaubey, I., Arnold, J.G., 2016. CMhyd User Manual. Available online: https://swat.tamu.edu/media/115265/bias_cor_man.pdf (Accessed on 16 October 2018). .

Riahi, K., Grübler, A., Nakicenovic, N., 2007. Scenarios of long-term socio-economic and environmental development under climate stabilization. Technol. Forecast. Soc. Change 74, 887–935.

Rojas, R., Feyen, L., Dosio, A., Bavera, D., 2011. Improving pan-European hydrological simulation of extreme events through statistical bias correction of RCM-driven climate simulations. Hydrol. Earth Syst. Sci. 15 (8), 2599–2620.

Rose, S.K., Ahammad, H., Eickhout, B., Fisher, B., Kurosawa, A., Rao, S., Riahi, K., van Vuuren, D.P., 2012. Land-based mitigation in climate stabilization. Energy Econ. 34 (1), 365–380.

Seager, R., Vecchi, G.A., 2010. Greenhouse warming and the 21st century hydroclimate of Southwestern North America. Proc. Natl. Acad. Sci. 107 (50), 21277–21282.

Sennikovs, J., Bethers, U., 2009. Statistical downscaling method of regional climate model results for hydrological modelling. In: Anderssen, R.S., Braddock, R.D., Newham, L.T.H. (Eds.), 18th World IMACS Congress and MODSIM09 International Congress on Modelling and Simulation. Modelling and Simulation Society of Australia and New Zealand and International Association for Mathematics and Computers in Simulation, pp. 3962–3968.

Shafer, M., Ojima, D., Antle, J.M., Kluck, D., McPherson, R.A., Petersen, S., Scanlon, B., Sherman, K., 2014. Ch. 19: Great Plains climate change impacts in the United States. Third Natl. Clim. Assess. (Accessed on 18 October 2018). https://www.sciencebase.gov/catalog/item/553e6894e4b0a658d7938957.

Smith, S.J., Wigley, T.M.L., 2006. Multi-gas forcing stabilization with minicam. Energ. J. 27, 373–392.

Sreeharsha, R.V., Sekhar, K.M., Reddy, A.R., 2015. Delayed flowering is associated with lack of photosynthetic acclimation in Pigeon pea (*Cajanus cajan* L.) grown under elevated CO_2. Plant Sci. 231, 82–93.

Stefanidis, K., Panagopoulos, Y., Mimikou, M., 2018. Response of a multi-stressed Mediterranean river to future climate and socio-economic scenarios. Sci. Total Environ. 627, 756–769.

Stewart, B.A., Steiner, J.L., 1990. Water-use efficiency. In: In: Stewart, B.A., Singh, R.P., Parr, J.F. (Eds.), Adv Soil Sci Vol 13. Springer Verlag, F.R.G., pp. 151–173.

Stewart, B.A., Musick, J.T., Dusek, D.A., 1983. Yield and water use efficiency of grain sorghum in a limited irrigation-dryland farming system. Agron. J. 75 (4), 629–634.

Suarez-Rey, E., Choi, C.Y., Waller, P.M., Kopec, D.M., 2000. Comparison of subsurface drip irrigation and sprinkler irrigation for Bermuda grass turf in Arizona. Trans. ASAE 43 (3), 631–640.

Sun, F., Roderick, M.L., Lim, W.H., Farquhar, G.D., 2011. Hydroclimatic projections for the Murray-Darling Basin based on an ensemble derived from Intergovernmental Panel on Climate Change AR4 climate models. Water Resour. Res. 47, W00G02.

Teutschbein, C., Seibert, J., 2010. Regional climate models for hydrological impact studies at the catchment scale: a review of recent modeling strategies. Geogr. Compass 4 (7), 834–860.

Unger, P.W., Pringle, F.B., 1981. Pullman Soils: Distribution Importance, Variability, and Management; Bulletin B-1372. Texas Agricultural Experiment Station, College Station, TX, USA.

United States Environmental Protection Agency (USEPA), 2019. Climate Change: Basic Information. Available online: http://www.epa.gov/climatechange/basics/ (Accessed on 14 October 2018). .

Van Vuuren, D.P., Eickhout, B., Lucas, P.L., den Elzen, M.G.J., 2006. Long-term multi-gas scenarios to stabilise radiative forcing-exploring costs and benefits within an integrated assessment framework. Energ. J. 27, 201–233.

Van Vuuren, D.P., Den Elzen, M.G.J., Lucas, P.L., Eickhout, B., Strengers, B.J., Van Ruijven, B., Wonink, S., Van Houdt, R., 2007. Stabilizing greenhouse gas concentrations at low levels: an assessment of reduction strategies and costs. Clim. Change 81, 119–159.

Van Vuuren, D.P., Stehfest, E., den Elzen, M.G., Kram, T., van Vliet, J., Deetman, S., Isaac, M., Goldewijk, K.K., Hof, A., Beltran, A.M., Oostenrijk, R., 2011. RCP2.6: exploring the possibility to keep global mean temperature increase below 2°C. Clim. Change 109 (1-2), 95–116.

Varis, O., Kajander, T., Lemmelä, R., 2004. Climate and water: from climate models to water resources management and vice versa. Clim. Change 66 (3), 321–344.

Verchot, L.V., Van Noordwijk, M., Kandji, S., Tomich, T., Ong, C., Albrecht, A., Mackensen, J., Bantilan, C., Anupama, K.V., Palm, C., 2007. Climate change: linking adaptation and mitigation through agroforestry. Mitig. Adapt. Strateg. Glob. Change 12 (5), 901–918.

Wang, R., Bowling, L.C., Cherkauer, K.A., Cibin, R., Her, Y., Chaubey, I., 2017. Biophysical and hydrological effects of future climate change including trends in CO_2, in the St. Joseph River watershed, Eastern Corn Belt. Agric. Water Manage. 180, 280–296.

Williams, A., White, N., Mushtaq, S., Cockfield, G., Power, B., Kouadio, L., 2015. Quantifying the response of cotton production in eastern Australia to climate change. Clim. Change 129 (1-2), 183–196.

Wise, M., Calvin, K., Thomson, A., Clarke, L., Bond-Lamberty, B., Sands, R., Smith, S.J., Janetos, A., Edmonds, J., 2009. Implications of limiting CO_2 concentrations for land use and energy. Science 324, 1183–1186.

Wu, Y., Liu, S., Gallant, A., 2012a. Predicting impacts of increased CO_2 and climate change on the water cycle and water quality in the Semiarid James River Basin of the Midwestern USA. Sci. Total Environ. 430, 150–160.

Wu, Y., Liu, S., Abdul-Aziz, O.I., 2012b. Hydrological effects of the increased CO_2 and climate change in the Upper Mississippi River Basin using a modified SWAT. Clim. Change 110 (3-4), 977–1003.

Xu, Z., Jiang, Y., Jia, B., Zhou, G., 2016. Elevated-CO_2 response of stomata and its dependence on environmental factors. Front. Plant Sci. 7, 657.

Ye, L., Grimm, N.B., 2013. Modelling potential impacts of climate change on water and nitrate export from a mid-sized, semiarid watershed in the US Southwest. Clim. Change 120 (1-2), 419–431.

Zhang, H., Mu, J.E., McCarl, B.A., 2017. Adaption to climate change through fallow rotation in the US Pacific Northwest. Climate 5 (3), 64.